quaternary

MDPI

Article

Synchronous or Not? The Timing of the Younger Dryas and Greenland Stadial-1 Reviewed Using Tephrochronology

Simon A. Larsson [1,2,*], Malin E. Kylander [2,3], A. Britta K. Sannel [1,2] and Dan Hammarlund [4]

[1] Department of Physical Geography, Stockholm University, 106 91 Stockholm, Sweden; britta.sannel@natgeo.su.se
[2] The Bolin Centre for Climate Research, Stockholm University, 106 91 Stockholm, Sweden; malin.kylander@geo.su.se
[3] Department of Geological Sciences, Stockholm University, 106 91 Stockholm, Sweden
[4] Department of Geology, Lund University, 223 62 Lund, Sweden; dan.hammarlund@geol.lu.se
* Correspondence: simon.larsson@natgeo.su.se

Abstract: The exact spatial and temporal behaviour of rapid climate shifts during the Last Glacial–Interglacial Transition are still not entirely understood. In order to investigate these events, it is necessary to have detailed palaeoenvironmental reconstructions at geographically spread study sites combined with reliable correlations between them. Tephrochronology, i.e., using volcanic ash deposits in geological archives as a dating and correlation tool, offers opportunities to examine the timing of events across wider regional scales. This study aims to review the posited asynchrony of the Younger Dryas stadial in comparison with Greenland Stadial-1 by correlating new proxy data from southernmost Sweden to previous palaeoclimate reconstructions in Europe based on the presence of the Hässeldalen Tephra, the Vedde Ash, and the Laacher See Tephra. μ-XRF core-scanning data were projected using a recently published age–depth model based on these tephras and several radiocarbon dates, and compared to previous findings, including by adapting previous chronologies to the recently proposed earlier date of the Laacher See Tephra (13,006 ± 9 cal. a BP). Although the results to some extent support the idea of a more synchronous Younger Dryas event than previously assumed, this issue requires further high-resolution proxy studies to overcome limitations of temporal precision.

Keywords: palaeoclimate; tephrostratigraphy; LGIT; Scandinavia; XRF; Hässeldalen Tephra; Vedde Ash; Laacher See Tephra

Citation: Larsson, S.A.; Kylander, M.E.; Sannel, A.B.K.; Hammarlund, D. Synchronous or Not? The Timing of the Younger Dryas and Greenland Stadial-1 Reviewed Using Tephrochronology. *Quaternary* **2022**, *5*, 19. https://doi.org/10.3390/quat5020019

Academic Editor: David J. Lowe

Received: 27 December 2021
Accepted: 2 March 2022
Published: 1 April 2022

1. Introduction

For a period of time after the Last Glacial Maximum (LGM, c. 22 ka [1]), when the last of the Eurasian and Laurentide ice sheets retreated, Earth experienced an unstable and disruptive climatic amelioration. Several rapid climate shifts occurred during what is often referred to as the Last Glacial–Interglacial Transition (LGIT, c. 16–8 ka [2]). A better understanding of these changes is important in Quaternary research, as these events, as recorded in geological archives, are still not entirely understood in terms of causes or timing [3–7]. Reconstructing the development of these changes in detail, across temporal and spatial scales, is crucial for improving our knowledge of the climate system of the past, which in turn is necessary for comprehending the behaviour of the climate in the present and the future [8].

A well-studied example of the uncertainties surrounding the timing of LGIT climate shifts is the onset of the Younger Dryas stadial (YD, climatostratigraphically defined at c. 12.8–11.6 ka [9]). This cold event has been attributed to major reconfigurations of the oceanic and atmospheric circulation in the North Atlantic beginning soon after 13 ka [10–16] and several hypotheses regarding its trigger have been put forward, including a large release of meltwater from the Laurentide Ice Sheet [17,18], a cosmic impact event [19,20], and volcanism [21–23]—though all of these have been contested [16,24,25].

When the YD has been used to define stratigraphic units in palaeoclimate reconstructions, an apparent asynchrony between locations and different climate proxies has been described; studies seem to demonstrate that both the timing and the duration of the YD varied in a geographically time-transgressive fashion in the North Atlantic region [26–32]. This also suggests that the YD was not synchronous with Greenland Stadial-1 (GS-1, the most recent stadial event recorded in the Greenland ice-core record and dated to 12,896–11,703 b2k [2]) and it has been recommended to not use the YD and GS-1 interchangeably [2,3].

The potential of tephrochronology as a correlation tool to test the synchroneity of past climate changes—with advantages in terms of temporal precision and spatial coverage—has already been extensively reviewed and demonstrated [33–47]. A number of tephras produced by eruptions during the LGIT are commonly found preserved in geological archives in Europe, such as the widespread Icelandic Vedde Ash [48] and the German Laacher See Tephra [49]; two key tephras in examining the timing of the YD. A recent study provided a refined, more precise date for the Laacher See Tephra based on a combination of dendrochronology and radiocarbon dating, which predates the previously accepted age estimate by more than 100 years [16]. This has implications for the posited asynchrony of the onset of the YD as interpreted in connection to occurrences of this tephra. Considering also the recent expansions of the geographical area where this tephra is discovered [50–53], it is now particularly important for the palaeoclimatic application of tephrochronology, and the new date calls for review of a number of previous studies.

With this in mind, we aim to examine the timing of LGIT climate shifts as interpreted based on terrestrial and lacustrine tephra deposits in Europe. We build upon a previous palaeoclimate reconstruction by Hammarlund & Lemdahl (1994) [54] and a new tephrostratigraphy and age model by Larsson & Wastegård (2022) [55] from Körslättamossen in southernmost Sweden with new high-resolution XRF core-scanning results to correlate our findings to other studies using the tephra deposits as isochrons. We find that there is evidence to support recent suggestions of a synchronous YD onset, but the question still requires further study as there are issues of comparability between sites and proxies as well as a need for more high-resolution palaeoclimate reconstructions with high-precision chronologies. The Körslättamossen sequence provides excellent opportunities for further research on this topic.

2. Materials and Methods

2.1. Fieldwork

The study site Körslättamossen is a small fen located in northwest Scania in southernmost Sweden (Figure 1). It is located at c. 118 m a.s.l. (which is c. 70 m above the highest coastline in the area [56]) and has a catchment of c. 750 ha underlain mainly by metamorphic bedrock (gneiss [57]). The fen was formed by terrestrialisation in a bedrock depression that held a small lake after deglaciation [54]. The area was deglaciated shortly after 17 ka [1], which means the site hosts one of the earliest post-LGM climate archives investigated in Scandinavia.

Parallel boreholes were cored at a location selected in an attempt to be as close as possible to the sampling location of the first study of the site [54]. Field notes from that study were used for in-field validation of the retrieved sediments. Russian corers [58] were used to collect a continuous stratigraphy by sampling cores with overlaps of 20–50 cm from the parallel boreholes. In total, nine sample cores were retrieved, covering depths 114–605 cm below the ground surface. The cores were wrapped in sheets of plastic and, upon return from the fieldwork, put into cold storage pending laboratory analyses.

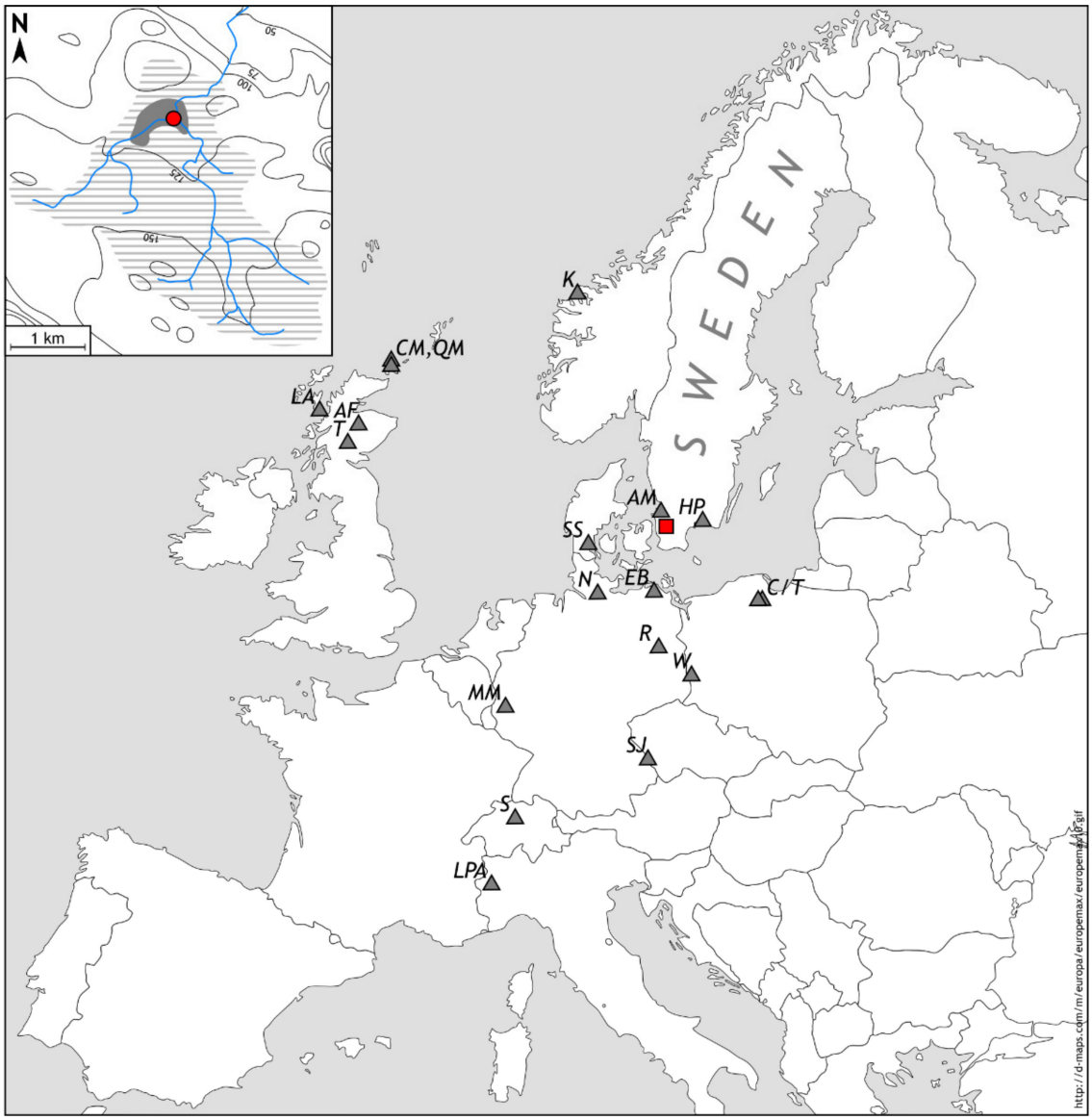

Figure 1. Locations of the study site Körslättamossen in southernmost Sweden (red square) and correlation sites (grey triangles): Abernethy Forest (AF) [59]; Atteköpsmosse (AM) [5,60]; Czechowskie/Trzechowskie (C/T) [31,61,62]; Crudale Meadow (CM) [63–65]; Endinger Bruch (EB) [66]; Hässeldala port (HP) [5,67–69]; Kråkenes (K) [70,71]; Lago Piccolo di Avigliana (LPA) [40,72]; Loch Ashik (LA) [59,73]; Meerfelder Maar (MM) [32,74,75]; Nahe (N) [53,76]; Quoyloo Meadow (QM) [77–79]; Rehwiese (R) [4]; Soppensee (S) [36,40,80–82]; Stará Jímka (SJ) [52,83]; Store Slotseng (SS) [84,85]; Tirinie (T) [6,86]; and Wegliny (W) [87]. Top-left inserted local map shows a simplified topography around the study site: coring location at 56°05′32.8″ N 13°03′50.0″ E (red circle); fen area (grey field); catchment area (striped field); streams (blue lines); and elevation as metres above sea level (solid lines). European map used for the main image from d-maps.com. Inserted map adapted from the first study of the site [54] based on a terrain map from Geological Survey of Sweden [88].

2.2. Labwork

2.2.1. μ-XRF Core Scanning

Prior to any subsampling, all sample cores were scanned in order to produce micro X-ray fluorescence (μ-XRF) elemental profiles using an ITRAX XRF Core Scanner [89] from Cox Analytical Systems (Gothenburg, Sweden) at the SLAM Laboratory, Department of Geological Sciences, Stockholm University, Sweden. Scanning was done on the flat sides

of the half-cylinder-shaped sample cores, which were scraped to even out the surfaces. Surfaces were covered with a thin Mylar plastic film to avoid drying of the cores during analysis. Scanning used a Mo tube set to 30 kV and 50 mA with a 1000 µm step size and 10 s exposure time. A composite core was created by selecting from the resulting raw counts, with cut-off points motivated by comparison to the stratigraphy and organic matter and carbon contents of the sediments, prioritising sequences with fewer invalid measurements and lower mean standard errors when possible. The data were investigated after smoothing by a 10-point running mean and log-ratio transformations (to overcome the issue of the constant-sum constraint [90–92]).

2.2.2. Carbon Content, Organic Matter, and Tephra Analysis

Further analyses employed are described in the recently published Körslättamossen study [55] and include: organic and carbonate carbon content analysis by an Eltra CS 500 Carbon Sulfur Determinator below 200 cm depth (the carbon content above this depth exceeded the instrument's detection levels); organic matter content measurement by loss-on-ignition (LOI [93]) above 200 cm depth; tephra extraction for microscopic examination following a procedure for extraction of rhyolitic glass from minerogenic sediments [94]; and re-extraction of tephra for geochemical analysis [95] at selected levels of peak concentrations. Extracted tephra shards were analysed using a Cameca SX-100 electron probe microanalyser (EPMA [96]) at the School of GeoSciences, University of Edinburgh, Scotland, UK.

2.2.3. Chronology

After the above, the remaining sample material was searched for terrestrial macrofossils suitable for radiocarbon dating. Selected samples were sent to the Tandem Laboratory, Uppsala University, Sweden, for accelerator mass-spectrometer analysis. The combined results of the tephra analysis and the radiocarbon age estimates gained were used to construct an age–depth model of the sampled sediments by Bayesian methods [97], and the results were used for projecting the proxy data against an age-scale. Dates are presented as calibrated years before present (i.e., before 1950 CE) unless otherwise noted.

3. Results and Discussion

3.1. Proxy Results and Age–Depth Modelling

The stratigraphy of the composite sediment sequence is divided into eleven units as described previously [55], building upon the first study of the site [54], and was defined mainly by the physical appearance of the sediments (Figure 2a). The age–depth model (Figure 2b) was based on a number of radiocarbon dates as well as the identifications of three tephras: the c. 11.3 ka Hässeldalen Tephra (HDT) [67]; the c. 12.0 ka Vedde Ash (VA) [48]; and the c. 13.0 ka Laacher See Tephra (LST) [49]. The organic matter and carbon content records (Figure 2c) agree well with the stratigraphic description, for example by the highest organic matter content being found in the topmost organic sediments and the lowest carbon content in the bottommost, purely minerogenic clays, and variations in-between being matched by sediment type and macrofossil contents.

The age–depth model used here is the presently best-available data for Körslättamossen, but it could be improved in terms of coverage as the topmost units 8–11 and bottommost unit 1 of the sediment sequence are only modelled by extrapolation of inferred accumulation rates. However, the age control in the interval between the bottommost radiocarbon dates and the HDT, i.e., units 2–7, are however considered precise enough for discussion of the timing of certain events (with the caveat of a wider error margin in units 2–6a—particularly in units 4–5, which correspond to a radiocarbon plateau). The available radiocarbon dates validate the identifications of the three tephras, which provide precise anchor points for detailed comparisons to other studies.

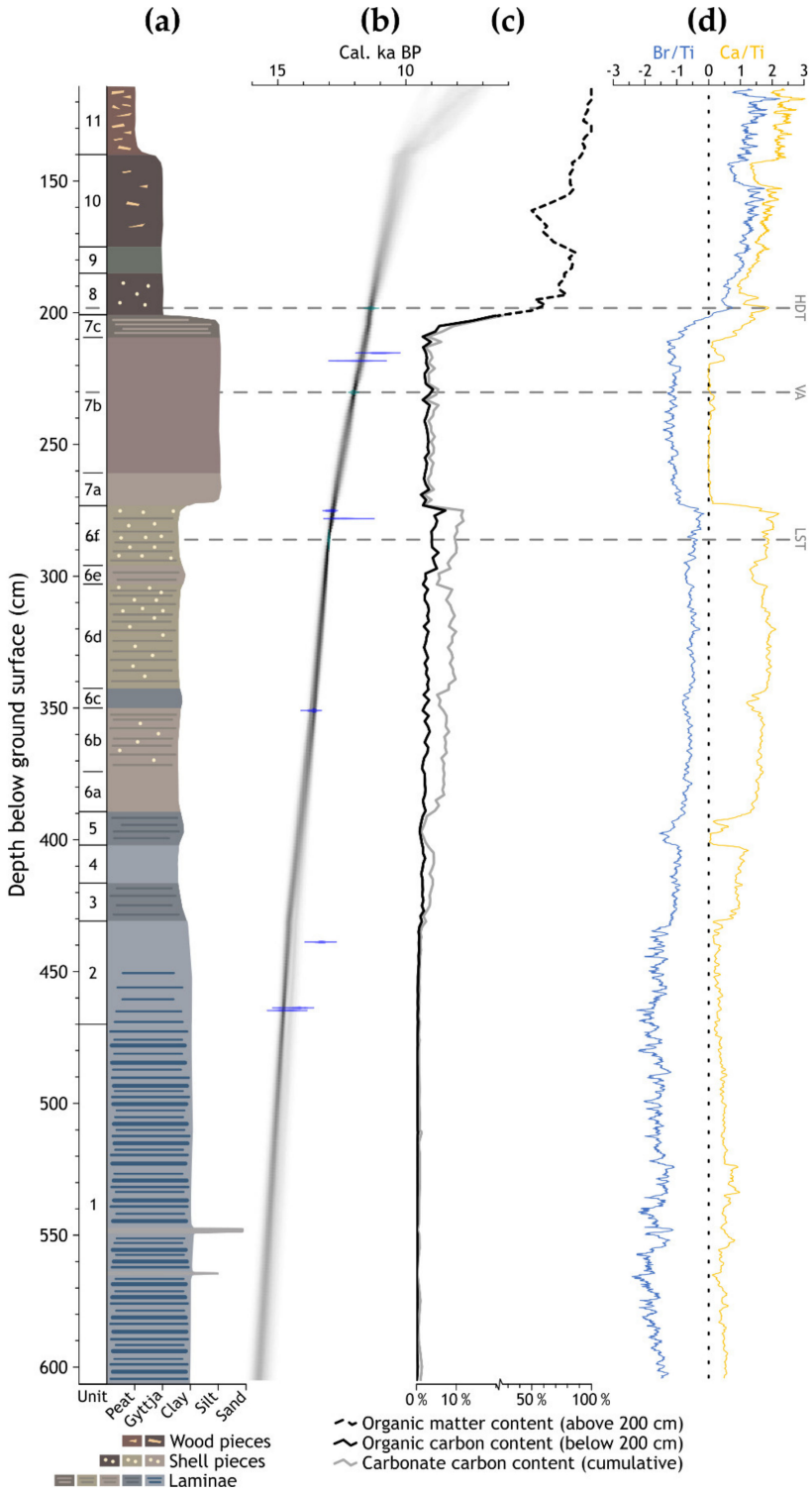

Figure 2. (**a**) Stratigraphy (unit numbers and simplified visualisation with colours resembling those of the sediments), (**b**) age–depth model (with radiocarbon dates indicated by blue error bars), and (**c**) organic matter and carbon contents (NB: broken axis) of the sampled sediment sequence, adapted from the recently published study of the site by Larsson & Wastegård (2022) [55]. (**d**) μ-XRF core-scanning results as selected log-ratio transformed elemental ratios (based on 10-point running means, dotted line shows 0 for reference). The positions of the Hässeldalen Tephra (HDT), the Vedde Ash (VA), and the Laacher See Tephra (LST) are indicated across the graph by dashed grey lines.

Based on analytical performance (counting statistics), reliable μ-XRF data was acquired for nearly the entire sediment sequence, interrupted only intermittently by single or a few contiguous analysis points annotated as invalid by the core scanner (see Supplementary Materials). The results were explored using log-ratio transformations of various elemental ratios. The overall variations of the Br/Ti and Ca/Ti ratios (Figure 2d) correspond well to the observed sediment type changes and the carbon record. As the Br/Ti ratio matches organic carbon, and bromine has previously been demonstrated to be closely connected to organic content [98,99], it is used here as an overall productivity proxy. Similarly, the Ca/Ti ratio matches carbonate carbon and high values coincide with units of calcareous gyttja and abundant shell macrofossils. Calcium is therefore interpreted to originate from the autochthonous, biogenic production of carbonates in the lake [27,100,101], as has also been demonstrated at the comparable site of Hässeldala port [102]. Titanium is considered a suitable normaliser for the log-ratio transformations of elements assumed to be connected to productivity as it is conservative and not involved in the biological processes.

From the XRF, organic matter, and carbon records, it can be interpreted that variations in climate affected the overall productivity in the postglacial palaeolake, and several rapid climate shifts can be recognised. For example, carbon contents and Br/Ti and Ca/Ti ratios sharply drop around the unit 6/7 boundary, where the sediments also shift from being rich in shells to being devoid of them, all indicating a significant change towards conditions which were less favourable for aquatic productivity. This likely reflects a shift to colder, stadial-like conditions similar to those immediately following deglaciation [54,55] and agrees with the previous suggestion that this unit boundary represents the onset of the YD [54]. Similarly, the transition from mainly minerogenic sediments to organic gyttja around the unit 7/8 boundary is reflected in the carbon contents and the Br/Ti and Ca/Ti ratios, as well. This transition has been attributed to the start of the Holocene [54].

Several more shifts are apparent from the proxy data. From unit 3 and through unit 6 there is a trend of slowly increasing organic and carbonate carbon contents matched by increasing values of the Br/Ti and Ca/Ti ratios, but there are several breaks in this trend that are also apparent as sediment-type changes. The most pronounced of these events, which are interpreted as representing shorter-term shifts to colder climatic conditions, correspond to units 5, 6c, and 6e, with unit 5 appearing the most significant. Here carbon contents are more or less depleted and the Br/Ti and Ca/Ti ratios revert to values matching those of the purely minerogenic clays of unit 1. Unit 5 was previously suggested to represent the Older Dryas stadial [54].

As we have performed μ-XRF core scanning on the same cores that have been examined for cryptotephra occurrences, we also have an opportunity to compare the results in order to briefly comment on the potential for XRF as a scanning tool for cryptotephra occurrences. Although the use of XRF has previously been successful in detecting visible tephra deposits [61,103–105] and in several cases cryptotephras [106–110]—and even to geochemically differentiate visible rhyolitic deposits [111]—low concentrations of rhyolitic cryptotephras often seem to evade detection [108,112]. At Körslättamossen, neither the rhyolitic HDT or VA nor the phonolitic LST correspond to any significant peak values in elements that have been used for cryptotephra detection. Despite the undeniable potential for tephra detection by XRF scanning in certain cases, we believe that our findings as well as previous evidence point to it not being completely reliable at distal locations.

Projecting the proxy data via the age–depth model (Figure 3) reveals a notable shift in resolution in different parts of the stratigraphy due to the varying accumulation rates of the sediments. For example, the results corresponding to the topmost 25 cm (unit 11) are stretched over what comprises almost a third of the sampled sequence in terms of age, while unit 1, the bottommost 135 cm, is compressed to just an eighth of the sequence. It should also be noted that while the original XRF data are of a millimetre-resolution, the projection is limited to the 1-cm resolution of the age–depth model. As the XRF data are handled as 10-point running means, this means that the data displayed in Figure 3d are in practice centimetre-averages. The parts of the Körslättamossen sequence which suffer from

less reliable age estimates are annotated by the red shading in Figure 3 and interpretations of the data in these parts are considered speculative.

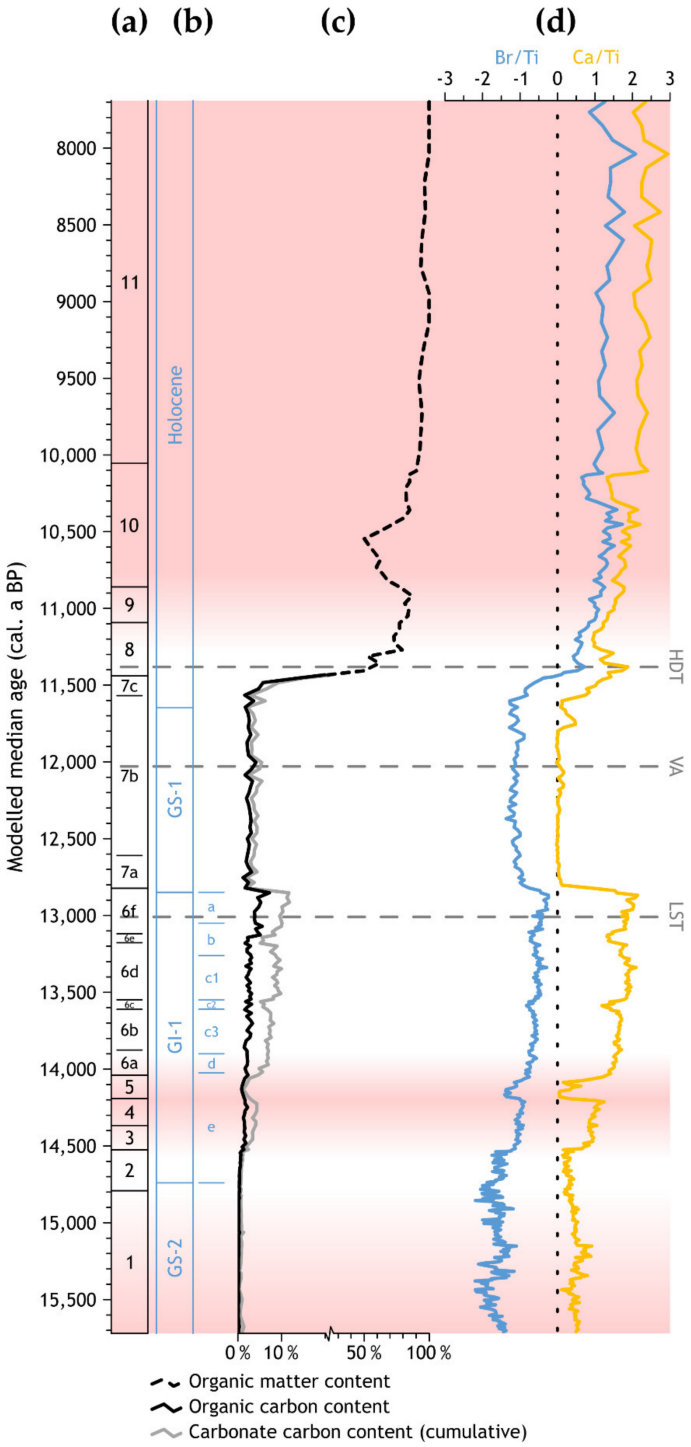

Figure 3. (**a**) Stratigraphic units, (**b**) Greenland ice-core record event stratigraphy [2], (**c**) organic matter and carbon contents (NB: broken axis), and (**d**) µ-XRF core-scanning results projected to modelled median ages from the age–depth model of the recently published study by Larsson & Wastegård (2022) [55] (as log-ratios of 10-point running means at a 1-cm resolution, dotted line shows 0 for reference). Red shading indicates where the age–depth model is less reliable. The positions of the Hässeldalen Tephra (HDT), the Vedde Ash (VA), and the Laacher See Tephra (LST) relative to the proxy results are indicated across the graph by dashed grey lines.

By comparison of the XRF data to the age–depth model, the unit 2/3 boundary at 431 cm, where productivity proxies start to display increasing trends, is assigned a median age of 14,525 cal. a BP (2σ-probability range 14,760–14,096 cal. a BP). The first reversal of this increase, that of unit 5 at 402–389 cm (the previously assumed Older Dryas unit) is dated to 14,193–14,040 cal. a BP, but this part of the age–model suffers from wide error margins (onset probability range 14,461–13,875, end 14,318–13,766). The following, less drastic reversals of units 6c and 6e, which by the XRF data can be defined at 353–346 and 304–295 cm, respectively, are dated to 13,637–13,571 cal. a BP (onset 13,855–13,498, end 13,789–13,428) and 13,192–13,108 cal. a BP (onset 13,391–13,075, end 13,295–13,029). These reversals appear to align somewhat well with the GI-1c2 and GI-1b events, as defined by Rasmussen et al. (2014) [2] (cf. Figure 3b).

The previously assumed onset of the YD near the unit 6/7 boundary can be defined by the XRF data at 275 cm; this is the point from which the Br/Ti and Ca/Ti ratios rapidly decrease to the stabilised, lower values found from c. 273 cm and upwards. The unit 6/7 boundary was defined at 273 cm by the sediment appearance in comparison to the carbon contents, the data of which is at a considerably lower resolution. The date for the onset of the YD is therefore defined here at 275 cm and is estimated to 12,853 cal. a BP (13,022–12,745). Likewise, the end of the YD can be defined at 212 cm, from where the Br/Ti and Ca/Ti ratios rise throughout unit 7c—similarly to the unit 6/7 boundary, the 7b/7c boundary was defined at 209 cm by comparison to the lower-resolution carbon content data. The end of the YD is therefore pinpointed here to 212 cm and is estimated to 11,623 cal. a BP (11,832–11,436).

A slight reversal in the rapidly increasing productivity connected to the start of the Holocene, at 198–194 cm (apparent from the organic matter contents as well as the Br/Ti and Ca/Ti ratios) is dated to 11,380–11,292 cal. a BP (onset 11,590–11,231, end 11,522–11,015) and is possibly comparable to the Preboreal Oscillation [113]. Another interesting reversal in the XRF data is found at 153–142 cm, in the top part of the gyttja of unit 10, before the transition to the fen peat of unit 11; here elemental ratios display a significant shift, which is only vaguely matched by the organic matter contents. This can only be dated by considerable extrapolation to 10,356–10,117 cal. a BP, and while the error margins are extensive (onset 10,816–9635, end 10,628–9338 cal. a BP), it is intriguing that extrapolation places this reversal as coincident with the "10.3 ka event" [114].

3.2. Timing of the Younger Dryas and Greenland Stadial-1

The timing of the YD at Körslättamossen as defined above implies a near-synchronous onset between southern Scandinavia and Greenland, where the start of the corresponding stadial GS-1 is defined in the ice-core record at 12,846 a BP (12,896 ± 4 b2k [2]). This is in contrast to previous suggestions of a time-transgressive YD onset in the North Atlantic region [5,29,30,34,45,69]. The end of the YD and transition into the Holocene is also estimated very close to the 11,653 cal. a BP (11,703 ± 4 b2k [2]) date of the end of the GS-1/start of the Holocene in the Greenland ice-core record. The Körslättamossen sequence therefore supports the idea of a synchronous YD onset as inferred from the new LST date [16].

To review the question of YD synchroneity further, a comparison was made with palaeoclimatic reconstructions over a wider region. As revealed by the high-resolution sampling approach, the tephras at Körslättamossen are found at clearly separated levels in the sediments with little-to-no background noise or intervening redeposited tephra shards [55]. Together with clearly pronounced maximum levels of shard concentrations, which allows confident identification of primary ashfall deposits, the HDT, VA, and LST therefore function as reliable isochrons for correlation. Their positions provide anchor points enveloping the YD, enabling comparisons to a selection of sites in Europe where these tephras have also been reported (see Figure 1).

A synthesis of the best available age estimates of the YD onset and end at comparison sites is provided in Table 1 and visualised in relation to the modelled ages from Körslätta-

mossen as well as the dates of Greenland Stadial-1 in Figure 4. For sites where the LST was identified before the new date of 13,006 ± 9 cal. a BP was reported [16] (and for which age models have used a previously accepted, younger date for this tephra—most commonly 12,880 varve years BP [74]), alternative YD onset ages are provided in Figure 4 by linear corrections of the time difference between the old and new LST dates. Admittedly, a reliably adjusted age estimate should be produced by performing new age models in full for each affected site, but such an undertaking is beyond the scope of this paper and is impossible for some sites where necessary raw data for reproducing the modelling approaches are not available.

Table 1. Best available age estimates of the Younger Dryas (YD) onset and end at the comparison sites, presented as expressed in the source and as cal. a BP unless otherwise noted. Tephras identified at each site are indicated by their abbreviations: the Hässeldalen Tephra (HDT); the Vedde Ash (VA); and the Laacher See Tephra (LST).

Country	Site	YD Onset	YD End	Tephras	References
Scotland	Loch Ashik	13,600 [a]	11,400 ± 773	VA	[59,73]
Scotland	Abernethy Forest	13,000 ± 610	11,550 ± 200	VA	[59]
Scotland	Tirinie	12,820 ± 290	11,710 ± 260	VA	[6,86]
Scotland	Crudale Meadow	12,990 ± 500	12,100–11,500 [a]	HDT, VA	[63–65]
Scotland	Quoyloo Meadow	13,120 ± 570	11,460 ± 220	HDT, VA	[77–79]
Norway	Kråkenes	12,737 ± 31	11,535 ± 58	VA	[70,71]
Sweden	Atteköpsmosse	12,900 [a]	11,500 [a]	HDT, VA	[5,60]
Sweden	Hässeldala port	12,931 ± 90	11,564 ± 158	HDT, VA	[5,67–69]
Denmark	Store Slotseng	12,405 ± 233	11,500 [b]	HDT, VA	[84,85]
Germany	Nahe	12,540 [b]	11,560 [b]	VA, LST	[53,76]
Germany	Endinger Bruch	12,679–12,212	12,138–11,631	HDT, VA, LST	[66]
Germany	Meerfelder Maar	12,679 [v]	11,590 [v]	VA, LST	[32,74,75]
Germany	Rehwiese	12,675 [v]	11,690 [v]	LST	[4]
Poland	Wegliny	12,626 ± 101	11,471 ± 85	HDT, LST	[87]
Poland	Czechowskie/Trzechowskie	12,678 [v]	11,540 [b]	LST	[31,61,62]
Czech Republic	Stará Jímka	12,727 ± 92 *	11,435 ± 221	LST	[52,83]
Switzerland	Soppensee	12,750–12,450	11,600–11,220	VA, LST	[36,40,80–82]
Italy	Lago Piccolo di Avigliana	12,900–12,500	n/a	VA, LST	[40,72]

[a] Age estimate not explicitly reported (interpreted here from available data in the source). [b] Age estimate reported without probability range specified. [v] Varve years BP. * Age estimate adjusted in an incompletely described fashion.

In this simple comparison, it becomes apparent that at the sites where the LST was detected, the shift in the age estimates of the YD onset when adjusting for the new date does push the ages into a near-synchronous timing compared to the Körslättamossen and Greenland ice-core records. Even though only a crude, linear adjustment is made here to test the idea, this is viable for the sites in Germany and Poland where varve ages are assigned to the YD onset by the counting of c. 200 varves between it and the LST [4,61,74,80]. It is also noted that in one study from the Trzechowskie site, radiocarbon ages of 12,726 ± 47 and 12,831 ± 120 cal. a BP at the YD onset were omitted from the age model [31] when in fact they align quite well with the LST-corrected age estimate.

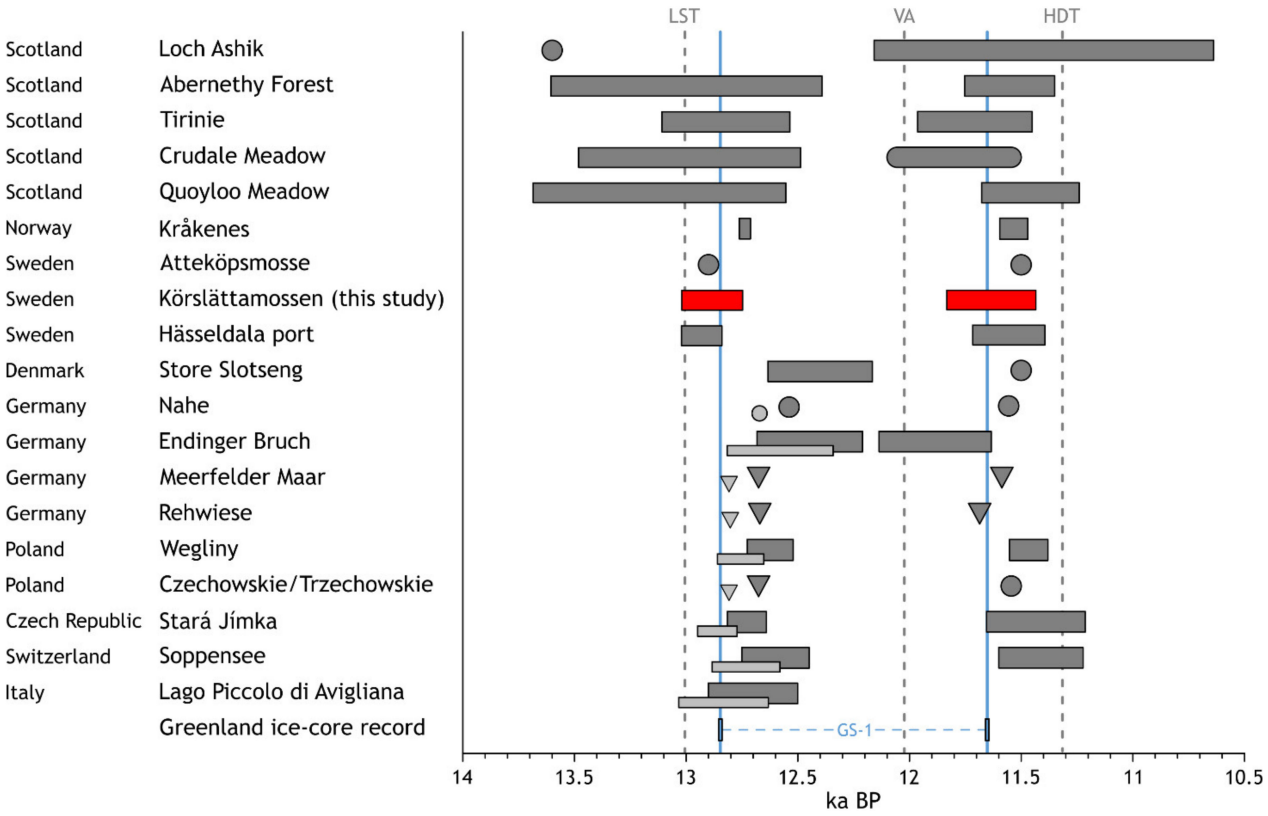

Figure 4. Visualisation of the best available age estimates of the onset and end of the Younger Dryas at the comparison sites (grey bars) and Körslättamossen (red bars) as well as of Greenland Stadial-1 (blue bars with dashed interval and vertical lines across the graph for onset and end). Bar widths represent probability ranges. Varve ages are shown as triangles. Note that age estimates shown as rounded bars are not explicitly reported in the source (instead interpreted from the available data) and that circles represent approximate ages without probability ranges. Alternative YD onset ages, linearly corrected by the new Laacher See Tephra date, are shown in light grey where applicable. For data used, see Table 1 and the text. Age estimates of the Hässeldalen Tephra (HDT), the Vedde Ash, and the Laacher See Tephra (LST) are indicated across the graph by dashed grey lines.

However, the corrected age estimates at the varve sites do not exactly match the GS-1 start date—a difference of c. 40 years remains. If this difference in time is considered of significant magnitude and taken as evidence of an asynchronous YD onset between Greenland and central Europe, it becomes obvious that the limited precision of radiocarbon ages and related modelling efforts are insufficient to precisely test the issue of synchroneity. If so, annually resolved records seem to be required for this purpose.

As for the possibility of a synchronised onset of the YD across Europe, only three sites—Loch Ashik, Store Slotseng, and Nahe—do not overlap with the modelled age range from Körslättamossen (after LST correction at Nahe). However, the date from Loch Ashik (c. 13,600 cal. a BP) is only an approximate age interpreted here from the results in the source [59] and the (uncorrected) date from Nahe (12,540 cal. a BP) is only reported as an approximate age without specified probability ranges. The late date for the onset of the YD at Store Slotseng (12,405 $\pm$ 233 cal. a BP) is based on only a single radiocarbon date at the YD onset sediment transition [85], which assigns a younger date than what was reported in a previous study of the site, where an older date (12,520 $\pm$ 102 cal. a BP) was obtained above the YD onset sediment transition [84].

The quite precise date from Kråkenes (12,737 $\pm$ 31 cal. a BP) overlaps only marginally with the probability range of the YD onset at Körslättamossen and is more difficult to dispute as it stems from a particularly robust age model [70]. With no trace of the LST

so far north as Norway, it appears still to indicate a difference in timing of the YD onset between western and southern Scandinavia (even when compared to recently recalibrated results [16]). If this is the case, it may yet support previous suggestions of atmospheric and oceanic shifts in the North Atlantic region being the causes for an asynchronous YD onset as reflected in palaeoclimate records [10,11,28,30,32].

As for the YD end, we note that all sites but one (Rehwiese) have age estimate probability ranges or approximates that overlap with the period 11,600–11,500 cal. a BP. There is considerable variation in the exact probabilities at each site (and several are not reported), but if it is any indication, it would suggest a slightly later YD end as reconstructed at European sites compared to the GS-1 end date (11,653 cal. a BP). However, this is highly speculative and requires proper re-modelling of age estimates to be examined any further.

Apart from contributing to age models with previously reported age estimates, the tephras provide isochrons for further examination of the timing of events across the sites. As the LST is consistently found below the YD sediments at all sites, it sets a limit for how early the YD onset can be. Therefore, some of the age estimates presented in Table 1 and Figure 4 can be additionally constrained. At Lago Piccolo di Avigliana and Körslättamossen, this can be assumed to push the earliest possible YD onset age estimate yet closer to the start of the GS-1. A suspected but unconfirmed LST presence at Hässeldala port [67] implies the same for this site. Similarly, the presence of the VA at Loch Ashik, Crudale Meadow, and Endinger Bruch limits the earliest possible YD end (as the VA appears within YD sediments and therefore well before any YD end estimate) and the presence of the HDT at Quoyloo Meadow limits the latest possible YD end compared to the available age estimates (as the HDT appears above YD sediments).

The results of this simple comparison and any possible conclusions drawn from them are complicated by a number of limitations of the source data. There is no properly standardised way of presenting age estimates or how they were calculated (for example, reporting mean or median ages, 1σ- or 2σ-probability ranges, presenting probability distributions clearly, describing modelling approaches sufficiently for reproduction, etc.), meaning that the types of ages used here are of varying character and quality. Furthermore, some radiocarbon ages were calibrated using what are by now outdated calibration curves, and the time period of interest here does have some significant differences even between the two most recent calibration curves [115]. Some palaeoclimate reconstructions did not, as mentioned, specify modelled or even approximate ages for the YD onset and/or end [59,60,63,76], and while other studies did, they may not have specified how such an age estimate was calculated [83], or motivated why one of several alternative age models was selected [68], or presented full dating data despite claiming to provide improved chronologies compared to previous studies of the same site [69]. Another issue is the complex relationship between different proxies and their possible lags in response to climatic changes [6], which has implications for the definition of a climatic event at a site before even attempting to assign age estimates for it. With all this taken into consideration, it becomes obvious that in addition to the need for more clearly presented, high-resolution proxy studies with high-precision chronologies, there is also a need for more sophisticated comparisons to approach a definitive solution to the issue of synchroneity of rapid climate changes during the LGIT.

3.3. Future Research Directions

To summarise, the question of whether the YD was synchronous or not in the North Atlantic region and with the GS-1 is not fully answered here. While there are clear indications that the posited asynchrony is not as obvious as previous interpretations of European proxy records have suggested, there are still issues to overcome to fully understand the timing of such climatic events in terms of temporal resolution and precision as well as their spatial correlation. Even though it was recently suggested that the YD and GS-1 were synchronised on a hemispheric scale [7], it remains difficult to prove such synchroneity even within Europe.

The natural archive of LGIT climate change available at Körslättamossen offers excellent possibilities for further investigation. The comparatively high-resolution and seemingly continuous sequence from the deglaciation into the Holocene, together with the cryptotephras identified (and additional ones yet to be determined [55]), as well as the fact that it can be successfully resampled and correlated to previous studies makes it an excellent study site. By applying additional proxy methods and improving the chronology further, Körslättamossen can be a key site in European palaeoclimate research.

The relationships between different proxies' responses to environmental changes must be properly considered for a complete understanding of the information provided in natural archives, and it is evident from the inter-site comparison attempted in this study that this is crucial for proper reviews of event chronologies across wider regions. Furthermore, validation of XRF results by multi-proxy approaches is particularly important as palaeoreconstructions based on XRF records may have no current analogue and can be biased by site-specific conditions [27,116]. With additional proxy analyses, the Körslättamossen sequence offers suitable study material for these issues.

The proxy results presented in this study also indicate environmental shifts in parts of the sequence that have yet to be properly examined, pending improved chronological control. At a first glance they appear to have a structure comparable to events in the Greenland ice-core record and other, regionally representative events. The Körslättamossen sequence could therefore be of importance for future investigation of these events, as well.

4. Conclusions

Tephrochronology offers a number of advantages in the investigation of the timing of past climate changes over wider regions. However, by our comparison based on European study sites where the Hässeldalen Tephra, the Vedde Ash, and/or the Laacher See Tephra have been identified, we find that further investigation is required to answer the question of whether the Younger Dryas was a synchronous event or not. The answer is yet obscured by dating uncertainties and complexities regarding the interpretation of palaeoclimate proxy data, and such matters must therefore be taken into strict consideration in future studies.

The Körslättamossen sequence in southernmost Sweden, with a growing proxy dataset and several occurrences of cryptotephra, offers excellent opportunities for such efforts, but annually laminated records may be required to achieve the temporal resolution necessary for accurate palaeoclimate reconstructions of rapid climate shifts.

Finally, we stress that clarity and transparency is vital when reporting age estimates and describing age–depth modelling approaches undertaken in palaeoclimate studies, as the risk of misinterpretation of such information can be detrimental for reviews of the timing of past climatic events.

Supplementary Materials: The following supporting information can be downloaded at: https://www.mdpi.com/article/10.3390/quat5020019/s1, Table S1: μ-XRF core-scanning results of the sampled sediments, presented as raw counts for each included element. Individual sample cores are separated by three empty rows. Edges at tops and bottoms of some sample cores, resulting in high MSE and/or low validity and interpreted as scanner beam hits on container materials, have been removed from the dataset. The total number of invalid measurements in the dataset is 103, representing c. 1.5% of the total number of analysis points. Table S2: Composite-core selection of μ-XRF results of the sampled sediments, presented as raw counts for each element. Zero-counts have been replaced by minimum values ($1E^{-19}$) in order to allow for log-ratio transformations. The number of invalid measurements included is 44, representing 0.4% of the total number of analysis points in the composite dataset. Table S3: Selected log-ratios of the composite core μ-XRF results, visualised in Figures 2 and 3 in the paper. Log-ratio transformations performed on 10-point running means of raw counts.

Author Contributions: Conceptualization, S.A.L.; methodology, S.A.L., M.E.K., A.B.K.S. and D.H.; software, S.A.L.; validation, S.A.L., M.E.K., A.B.K.S. and D.H.; formal analysis, S.A.L. and M.E.K.; investigation, S.A.L.; resources, M.E.K. and A.B.K.S.; data curation, S.A.L. and M.E.K.; writing—original draft preparation, S.A.L.; writing—review and editing, S.A.L., M.E.K., A.B.K.S. and D.H.; visualisation, S.A.L.; supervision, A.B.K.S.; project administration, S.A.L.; funding acquisition, S.A.L. All authors have read and agreed to the published version of the manuscript.

Funding: This research was funded by Vetenskapsrådet (the Swedish Research Council), grant number 2015-05255 (awarded to Stefan Wastegård), and by the Bolin Centre for Climate Research via various small grants (awarded to Simon Larsson) without grant numbers. The APC was funded by the Stockholm University Library.

Institutional Review Board Statement: Not applicable.

Informed Consent Statement: Not applicable.

Data Availability Statement: The data presented in this study are available in the Supplementary Materials and in referenced previous studies.

Acknowledgments: The authors would like to thank Stefan Wastegård and Helene Sunmark for their aid during the fieldwork as well as Chris Hayward and Maarten Blaauw for their helpful support in the work which this study builds upon. This research was conducted as part of Simon Larsson's doctoral project, the funding of which was obtained by his main supervisor Stefan Wastegård.

Conflicts of Interest: The authors declare no conflict of interest. The funders had no role in the design of the study; in the collection, analyses, or interpretation of data; in the writing of the manuscript, or in the decision to publish the results.

References

1. Stroeven, A.P.; Hättestrand, C.; Kleman, J.; Heyman, J.; Fabel, D.; Fredin, O.; Goodfellow, B.W.; Harbor, J.M.; Jansen, J.D.; Olsen, L.; et al. Deglaciation of Fennoscandia. *Quat. Sci. Rev.* **2016**, *147*, 91–121. [CrossRef]
2. Rasmussen, S.O.; Bigler, M.; Blockley, S.P.; Blunier, T.; Buchardt, S.L.; Clausen, H.B.; Cvijanovic, I.; Dahl-Jensen, D.; Johnsen, S.J.; Fischer, H.; et al. A Stratigraphic Framework for Abrupt Climatic Changes during the Last Glacial Period Based on Three Synchronized Greenland Ice-Core Records: Refining and Extending the INTIMATE Event Stratigraphy. *Quat. Sci. Rev.* **2014**, *106*, 14–28. [CrossRef]
3. Lowe, J.J.; Rasmussen, S.O.; Björck, S.; Hoek, W.Z.; Steffensen, J.P.; Walker, M.J.C.; Yu, Z.C. Synchronisation of Palaeoenvironmental Events in the North Atlantic Region during the Last Termination: A Revised Protocol Recommended by the INTIMATE Group. *Quat. Sci. Rev.* **2008**, *27*, 6–17. [CrossRef]
4. Neugebauer, I.; Brauer, A.; Dräger, N.; Dulski, P.; Wulf, S.; Plessen, B.; Mingram, J.; Herzschuh, U.; Brande, A. A Younger Dryas Varve Chronology from the Rehwiese Palaeolake Record in NE-Germany. *Quat. Sci. Rev.* **2012**, *36*, 91–102. [CrossRef]
5. Schenk, F.; Wohlfarth, B. *The Imprint of Hemispheric-Scale Climate Transitions on the European Climate during the Last Deglaciation (15.9 Ka to 9 Ka BP)*; Swedish Nuclear Fuel and Waste Management Co.: Stockholm, Sweden, 2019; pp. 1–98.
6. Abrook, A.M.; Matthews, I.P.; Candy, I.; Palmer, A.P.; Francis, C.P.; Turner, L.; Brooks, S.J.; Self, A.E.; Milner, A.M. Complexity and Asynchrony of Climatic Drivers and Environmental Responses during the Last Glacial-Interglacial Transition (LGIT) in North-West Europe. *Quat. Sci. Rev.* **2020**, *250*, 106634. [CrossRef]
7. Nakagawa, T.; Tarasov, P.; Staff, R.; Bronk Ramsey, C.; Marshall, M.; Schlolaut, G.; Bryant, C.; Brauer, A.; Lamb, H.; Haraguchi, T.; et al. The Spatio-Temporal Structure of the Lateglacial to Early Holocene Transition Reconstructed from the Pollen Record of Lake Suigetsu and Its Precise Correlation with Other Key Global Archives: Implications for Palaeoclimatology and Archaeology. *Glob. Planet. Change* **2021**, *202*, 103493. [CrossRef]
8. Tierney, J.E.; Poulsen, C.J.; Montañez, I.P.; Bhattacharya, T.; Feng, R.; Ford, H.L.; Hönisch, B.; Inglis, G.N.; Petersen, S.V.; Sagoo, N.; et al. Past Climates Inform Our Future. *Science* **2020**, *370*, 680. [CrossRef]
9. Mangerud, J. The Discovery of the Younger Dryas, and Comments on the Current Meaning and Usage of the Term. *Boreas* **2021**, *50*, 1–5. [CrossRef]
10. Sirocko, F.; Martínez-García, A.; Mudelsee, M.; Albert, J.; Britzius, S.; Christl, M.; Diehl, D.; Diensberg, B.; Friedrich, R.; Fuhrmann, F.; et al. Muted Multidecadal Climate Variability in Central Europe during Cold Stadial Periods. *Nat. Geosci.* **2021**, *14*, 651–658. [CrossRef]
11. Brauer, A.; Haug, G.H.; Dulski, P.; Sigman, D.M.; Negendank, J.F.W. An Abrupt Wind Shift in Western Europe at the Onset of the Younger Dryas Cold Period. *Nat. Geosci.* **2008**, *1*, 520–523. [CrossRef]
12. Bakke, J.; Lie, Ø.; Heegaard, E.; Dokken, T.; Haug, G.H.; Birks, H.H.; Dulski, P.; Nilsen, T. Rapid Oceanic and Atmospheric Changes during the Younger Dryas Cold Period. *Nat. Geosci.* **2009**, *2*, 202–205. [CrossRef]

13. Pearce, C.; Seidenkrantz, M.-S.; Kuijpers, A.; Massé, G.; Reynisson, N.F.; Kristiansen, S.M. Ocean Lead at the Termination of the Younger Dryas Cold Spell. *Nat. Commun.* **2013**, *4*, 1664. [CrossRef] [PubMed]
14. Schenk, F.; Väliranta, M.; Muschitiello, F.; Tarasov, L.; Heikkilä, M.; Björck, S.; Brandefelt, J.; Johansson, A.V.; Näslund, J.-O.; Wohlfarth, B. Warm Summers during the Younger Dryas Cold Reversal. *Nat. Commun.* **2018**, *9*, 1634. [CrossRef]
15. Cheng, H.; Zhang, H.; Spötl, C.; Baker, J.; Sinha, A.; Li, H.; Bartolomé, M.; Moreno, A.; Kathayat, G.; Zhao, J.; et al. Timing and Structure of the Younger Dryas Event and Its Underlying Climate Dynamics. *Proc. Natl. Acad. Sci. USA* **2020**, *117*, 23408–23417. [CrossRef]
16. Reinig, F.; Wacker, L.; Jöris, O.; Oppenheimer, C.; Guidobaldi, G.; Nievergelt, D.; Adolphi, F.; Cherubini, P.; Engels, S.; Esper, J.; et al. Precise Date for the Laacher See Eruption Synchronizes the Younger Dryas. *Nature* **2021**, *595*, 66–69. [CrossRef] [PubMed]
17. Broecker, W.S.; Kennett, J.P.; Flower, B.P.; Teller, J.T.; Trumbore, S.; Bonani, G.; Wolfli, W. Routing of Meltwater from the Laurentide Ice Sheet during the Younger Dryas Cold Episode. *Nature* **1989**, *341*, 318–321. [CrossRef]
18. Teller, J.T. Importance of Freshwater Injections into the Arctic Ocean in Triggering the Younger Dryas Cooling. *Proc. Natl. Acad. Sci. USA* **2012**, *109*, 19880–19881. [CrossRef]
19. Firestone, R.B.; West, A.; Kennett, J.P.; Becker, L.; Bunch, T.E.; Revay, Z.S.; Schultz, P.H.; Belgya, T.; Kennett, D.J.; Erlandson, J.M.; et al. Evidence for an Extraterrestrial Impact 12,900 Years Ago That Contributed to the Megafaunal Extinctions and the Younger Dryas Cooling. *Proc. Natl. Acad. Sci. USA* **2007**, *104*, 16016–16021. [CrossRef]
20. Sweatman, M.B. The Younger Dryas Impact Hypothesis: Review of the Impact Evidence. *Earth-Sci. Rev.* **2021**, *218*, 103677. [CrossRef]
21. Baales, M.; Jöris, O.; Street, M.; Bittmann, F.; Weninger, B.; Wiethold, J. Impact of the Late Glacial Eruption of the Laacher See Volcano, Central Rhineland, Germany. *Quat. Res.* **2002**, *58*, 273–288. [CrossRef]
22. Baldini, J.U.L.; Brown, R.J.; Mawdsley, N. Evaluating the Link between the Sulfur-Rich Laacher See Volcanic Eruption and the Younger Dryas Climate Anomaly. *Clim. Past* **2018**, *14*, 969–990. [CrossRef]
23. Abbott, P.M.; Niemeier, U.; Timmreck, C.; Riede, F.; McConnell, J.R.; Severi, M.; Fischer, H.; Svensson, A.; Toohey, M.; Reinig, F.; et al. Volcanic Climate Forcing Preceding the Inception of the Younger Dryas: Implications for Tracing the Laacher See Eruption. *Quat. Sci. Rev.* **2021**, *274*, 107260. [CrossRef]
24. Lowell, T.; Waterson, N.; Fisher, T.; Loope, H.; Glover, K.; Comer, G.; Hajdas, I.; Denton, G.; Schaefer, J.; Rinterknecht, V.; et al. Testing the Lake Agassiz Meltwater Trigger for the Younger Dryas. *Eos* **2005**, *86*, 365–372. [CrossRef]
25. Pinter, N.; Scott, A.C.; Daulton, T.L.; Podoll, A.; Koeberl, C.; Anderson, R.S.; Ishman, S.E. The Younger Dryas Impact Hypothesis: A Requiem. *Earth-Sci. Rev.* **2011**, *106*, 247–264. [CrossRef]
26. Lotter, A.F.; Birks, H.J.B.; Zolitschka, B. Late-Glacial Pollen and Diatom Changes in Response to Two Different Environmental Perturbations: Volcanic Eruption and Younger Dryas Cooling. *J. Paleolimnol.* **1995**, *14*, 23–47. [CrossRef]
27. Kylander, M.E.; Ampel, L.; Wohlfarth, B.; Veres, D. High-Resolution X-Ray Fluorescence Core Scanning Analysis of Les Echets (France) Sedimentary Sequence: New Insights from Chemical Proxies. *J. Quat. Sci.* **2011**, *26*, 109–117. [CrossRef]
28. Lane, C.S.; Brauer, A.; Blockley, S.P.E.; Dulski, P. Volcanic Ash Reveals Time-Transgressive Abrupt Climate Change during the Younger Dryas. *Geology* **2013**, *41*, 1251–1254. [CrossRef]
29. Rach, O.; Brauer, A.; Wilkes, H.; Sachse, D. Delayed Hydrological Response to Greenland Cooling at the Onset of the Younger Dryas in Western Europe. *Nat. Geosci.* **2014**, *7*, 109–112. [CrossRef]
30. Muschitiello, F.; Wohlfarth, B. Time-Transgressive Environmental Shifts across Northern Europe at the Onset of the Younger Dryas. *Quat. Sci. Rev.* **2015**, *109*, 49–56. [CrossRef]
31. Aichner, B.; Ott, F.; Słowiński, M.; Noryśkiewicz, A.M.; Brauer, A.; Sachse, D. Leaf Wax N-Alkane Distributions Record Ecological Changes during the Younger Dryas at Trzechowskie Paleolake (Northern Poland) without Temporal Delay. *Clim. Past* **2018**, *14*, 1607–1624. [CrossRef]
32. Obreht, I.; Wörmer, L.; Brauer, A.; Wendt, J.; Alfken, S.; De Vleeschouwer, D.; Elvert, M.; Hinrichs, K.-U. An Annually Resolved Record of Western European Vegetation Response to Younger Dryas Cooling. *Quat. Sci. Rev.* **2020**, *231*, 106198. [CrossRef]
33. Turney, C.S.M.; Harkness, D.D.; Lowe, J.J. The Use of Microtephra Horizons to Correlate Late-Glacial Lake Sediment Successions in Scotland. *J. Quat. Sci.* **1997**, *12*, 525–531. [CrossRef]
34. Lowe, J.J. Abrupt Climatic Changes in Europe during the Last Glacial–Interglacial Transition: The Potential for Testing Hypotheses on the Synchroneity of Climatic Events Using Tephrochronology. *Glob. Planet. Change* **2001**, *30*, 73–84. [CrossRef]
35. Turney, C.S.M.; Den Burg, K.V.; Wastegård, S.; Davies, S.M.; Whitehouse, N.J.; Pilcher, J.R.; Callaghan, C. North European Last Glacial–Interglacial Transition (LGIT; 15–9 Ka) Tephrochronology: Extended Limits and New Events. *J. Quat. Sci.* **2006**, *21*, 335–345. [CrossRef]
36. Lane, C.S.; Blockley, S.P.E.; Bronk Ramsey, C.; Lotter, A.F. Tephrochronology and Absolute Centennial Scale Synchronisation of European and Greenland Records for the Last Glacial to Interglacial Transition: A Case Study of Soppensee and NGRIP. *Quat. Int.* **2011**, *246*, 145–156. [CrossRef]
37. Lowe, D.J. Tephrochronology and Its Application: A Review. *Quat. Geochronol.* **2011**, *6*, 107–153. [CrossRef]
38. Abbott, P.M.; Davies, S.M. Volcanism and the Greenland Ice-Cores: The Tephra Record. *Earth-Sci. Rev.* **2012**, *115*, 173–191. [CrossRef]
39. Davies, S.M.; Abbott, P.M.; Pearce, N.J.G.; Wastegård, S.; Blockley, S.P.E. Integrating the INTIMATE Records Using Tephrochronology: Rising to the Challenge. *Quat. Sci. Rev.* **2012**, *36*, 11–27. [CrossRef]

40. Lane, C.S.; Blockley, S.P.E.; Lotter, A.F.; Finsinger, W.; Filippi, M.L.; Matthews, I.P. A Regional Tephrostratigraphic Framework for Central and Southern European Climate Archives during the Last Glacial to Interglacial Transition: Comparisons North and South of the Alps. *Quat. Sci. Rev.* **2012**, *36*, 50–58. [CrossRef]
41. Davies, S.M. Cryptotephras: The Revolution in Correlation and Precision Dating. *J. Quat. Sci.* **2015**, *30*, 114–130. [CrossRef]
42. Lowe, J.J.; Ramsey, C.B.; Housley, R.A.; Lane, C.S.; Tomlinson, E.L. The RESET Project: Constructing a European Tephra Lattice for Refined Synchronisation of Environmental and Archaeological Events during the Last c. 100 Ka. *Quat. Sci. Rev.* **2015**, *118*, 1–17. [CrossRef]
43. Lane, C.S.; Lowe, D.J.; Blockley, S.P.E.; Suzuki, T.; Smith, V.C. Advancing Tephrochronology as a Global Dating Tool: Applications in Volcanology, Archaeology, and Palaeoclimatic Research. *Quat. Geochronol.* **2017**, *40*, 1–7. [CrossRef]
44. Lowe, D.J.; Pearce, N.J.G.; Jorgensen, M.A.; Kuehn, S.C.; Tryon, C.A.; Hayward, C.L. Correlating Tephras and Cryptotephras Using Glass Compositional Analyses and Numerical and Statistical Methods: Review and Evaluation. *Quat. Sci. Rev.* **2017**, *175*, 1–44. [CrossRef]
45. Timms, R.G.O.; Matthews, I.P.; Lowe, J.J.; Palmer, A.P.; Weston, D.J.; MacLeod, A.; Blockley, S.P.E. Establishing Tephrostratigraphic Frameworks to Aid the Study of Abrupt Climatic and Glacial Transitions: A Case Study of the Last Glacial-Interglacial Transition in the British Isles (c. 16-8 Ka BP). *Earth-Sci. Rev.* **2019**, *192*, 34–64. [CrossRef]
46. Abbott, P.M.; Jensen, B.J.L.; Lowe, D.J.; Suzuki, T.; Veres, D. Crossing New Frontiers: Extending Tephrochronology as a Global Geoscientific Research Tool. *J. Quat. Sci.* **2020**, *35*, 1–8. [CrossRef]
47. Reinig, F.; Cherubini, P.; Engels, S.; Esper, J.; Guidobaldi, G.; Jöris, O.; Lane, C.; Nievergelt, D.; Oppenheimer, C.; Park, C.; et al. Towards a Dendrochronologically Refined Date of the Laacher See Eruption around 13,000 Years Ago. *Quat. Sci. Rev.* **2020**, *229*, 106128. [CrossRef]
48. Mangerud, J.; Lie, S.E.; Furnes, H.; Kristiansen, I.L.; Lømo, L. A Younger Dryas Ash Bed in Western Norway, and Its Possible Correlations with Tephra in Cores from the Norwegian Sea and the North Atlantic. *Quat. Res.* **1984**, *21*, 85–104. [CrossRef]
49. Van den Bogaard, P.; Schmincke, H.-U. Laacher See Tephra: A Widespread Isochronous Late Quaternary Tephra Layer in Central and Northern Europe. *Geol. Soc. Am. Bull.* **1985**, *96*, 1554–1571. [CrossRef]
50. Larsson, S.A.; Wastegård, S. The Laacher See Tephra Discovered in Southernmost Sweden. *J. Quat. Sci.* **2018**, *33*, 477–481. [CrossRef]
51. Kletetschka, G.; Vondrák, D.; Hruba, J.; van der Knaap, W.O.; van Leeuwen, J.F.N.; Heurich, M. Laacher See Tephra Discovered in the Bohemian Forest, Germany, East of the Eruption. *Quat. Geochronol.* **2019**, *51*, 130–139. [CrossRef]
52. Procházka, V.; Mizera, J.; Kletetschka, G.; Vondrák, D. Late Glacial Sediments of the Stará Jímka Paleolake and the First Finding of Laacher See Tephra in the Czech Republic. *Int. J. Earth Sci.* **2019**, *108*, 357–378. [CrossRef]
53. Krüger, S.; van den Bogaard, C. Small Shards and Long Distances—Three Cryptotephra Layers from the Nahe Palaeolake Including the First Discovery of Laacher See Tephra in Schleswig-Holstein (Germany). *J. Quat. Sci.* **2021**, *36*, 8–19. [CrossRef]
54. Hammarlund, D.; Lemdahl, G. A Late Weichselian Stable Isotope Stratigraphy Compared with Biostratigraphical Data: A Case Study from Southern Sweden. *J. Quat. Sci.* **1994**, *9*, 13–31. [CrossRef]
55. Larsson, S.A.; Wastegård, S. A High-Resolution Lateglacial–Early Holocene Tephrostratigraphy from Southernmost Sweden with Comments on the Borrobol–Penifiler Tephra Complex. *Quat. Geochronol.* **2022**, *67*, 101239. [CrossRef]
56. Fredén, C. *Sveriges Nationalatlas: Berg Och Jord*; Kartförlaget: Gävle, Sweden, 2009.
57. Geological Survey of Sweden. *Berggrund 1:50 000-1:250 000*; Sveriges Geologiska Undersökning: Uppsala, Sweden, 2017.
58. Jowsey, P.C. An Improved Peat Sampler. *New Phytol.* **1966**, *65*, 245–248. [CrossRef]
59. Brooks, S.J.; Matthews, I.P.; Birks, H.H.; Birks, H.J.B. High Resolution Lateglacial and Early-Holocene Summer Air Temperature Records from Scotland Inferred from Chironomid Assemblages. *Quat. Sci. Rev.* **2012**, *41*, 67–82. [CrossRef]
60. Wohlfarth, B.; Luoto, T.P.; Muschitiello, F.; Väliranta, M.; Björck, S.; Davies, S.M.; Kylander, M.; Ljung, K.; Reimer, P.J.; Smittenberg, R.H. Climate and Environment in Southwest Sweden 15.5–11.3 Cal. Ka BP. *Boreas* **2018**, *47*, 687–710. [CrossRef]
61. Wulf, S.; Ott, F.; Słowiński, M.; Noryśkiewicz, A.M.; Dräger, N.; Martin-Puertas, C.; Czymzik, M.; Neugebauer, I.; Dulski, P.; Bourne, A.J.; et al. Tracing the Laacher See Tephra in the Varved Sediment Record of the Trzechowskie Palaeolake in Central Northern Poland. *Quat. Sci. Rev.* **2013**, *76*, 129–139. [CrossRef]
62. Ott, F.; Wulf, S.; Serb, J.; Słowiński, M.; Obremska, M.; Tjallingii, R.; Błaszkiewicz, M.; Brauer, A. Constraining the Time Span between the Early Holocene Hässeldalen and Askja-S Tephras through Varve Counting in the Lake Czechowskie Sediment Record, Poland. *J. Quat. Sci.* **2016**, *31*, 103–113. [CrossRef]
63. Whittington, G.; Edwards, K.J.; Zanchetta, G.; Keen, D.H.; Bunting, M.J.; Fallick, A.E.; Bryant, C.L. Lateglacial and Early Holocene Climates of the Atlantic Margins of Europe: Stable Isotope, Mollusc and Pollen Records from Orkney, Scotland. *Quat. Sci. Rev.* **2015**, *122*, 112–130. [CrossRef]
64. Timms, R.G.O.; Matthews, I.P.; Palmer, A.P.; Candy, I. Toward a Tephrostratigraphic Framework for the British Isles: A Last Glacial to Interglacial Transition (LGIT c. 16-8 Ka) Case Study from Crudale Meadow, Orkney. *Quat. Geochronol.* **2018**, *46*, 28–44. [CrossRef]
65. Francis, C.P.; Engels, S.; Matthews, I.P.; Palmer, A.P.; Timms, R.G.O.; Jourdan, A.; Candy, I. A Multi-proxy Record of Abrupt Cooling Events during the Windermere Interstadial at Crudale Meadow, Orkney, UK. *J. Quat. Sci.* **2021**, *36*, 325–338. [CrossRef]
66. Lane, C.S.; De Klerk, P.; Cullen, V.L. A Tephrochronology for the Lateglacial Palynological Record of the Endinger Bruch (Vorpommern, North-East Germany). *J. Quat. Sci.* **2012**, *27*, 141–149. [CrossRef]

67. Davies, S.M.; Wastegård, S.; Wohlfarth, B. Extending the Limits of the Borrobol Tephra to Scandinavia and Detection of New Early Holocene Tephras. *Quat. Res.* **2003**, *59*, 345–352. [CrossRef]
68. Wohlfarth, B.; Blaauw, M.; Davies, S.M.; Andersson, M.; Wastegård, S.; Hormes, A.; Possnert, G. Constraining the Age of Lateglacial and Early Holocene Pollen Zones and Tephra Horizons in Southern Sweden with Bayesian Probability Methods. *J. Quat. Sci.* **2006**, *21*, 321–334. [CrossRef]
69. Wohlfarth, B.; Muschitiello, F.; Greenwood, S.L.; Andersson, A.; Kylander, M.; Smittenberg, R.H.; Steinthorsdottir, M.; Watson, J.; Whitehouse, N.J. Hässeldala—A Key Site for Last Termination Climate Events in Northern Europe. *Boreas* **2017**, *46*, 143–161. [CrossRef]
70. Lohne, Ø.S.; Mangerud, J.; Birks, H.H. Precise 14C Ages of the Vedde and Saksunarvatn Ashes and the Younger Dryas Boundaries from Western Norway and Their Comparison with the Greenland Ice Core (GICC05) Chronology. *J. Quat. Sci.* **2013**, *28*, 490–500. [CrossRef]
71. Lohne, Ø.S.; Mangerud, J.; Birks, H.H. IntCal13 Calibrated Ages of the Vedde and Saksunarvatn Ashes and the Younger Dryas Boundaries from Kråkenes, Western Norway. *J. Quat. Sci.* **2014**, *29*, 506–507. [CrossRef]
72. Finsinger, W.; Lane, C.S.; van Den Brand, G.J.; Wagner-Cremer, F.; Blockley, S.P.E.; Lotter, A.F. The Lateglacial Quercus Expansion in the Southern European Alps: Rapid Vegetation Response to a Late Allerød Climate Warming? *J. Quat. Sci.* **2011**, *26*, 694–702. [CrossRef]
73. Davies, S.M.; Turney, C.S.M.; Lowe, J.J. Identification and Significance of a Visible, Basalt-Rich Vedde Ash Layer in a Late-Glacial Sequence on the Isle of Skye, Inner Hebrides, Scotland. *J. Quat. Sci.* **2001**, *16*, 99–104. [CrossRef]
74. Brauer, A.; Endres, C.; Günter, C.; Litt, T.; Stebich, M.; Negendank, J.F.W. High Resolution Sediment and Vegetation Responses to Younger Dryas Climate Change in Varved Lake Sediments from Meerfelder Maar, Germany. *Quat. Sci. Rev.* **1999**, *18*, 321–329. [CrossRef]
75. Lane, C.S.; Brauer, A.; Martín-Puertas, C.; Blockley, S.P.E.; Smith, V.C.; Tomlinson, E.L. The Late Quaternary Tephrostratigraphy of Annually Laminated Sediments from Meerfelder Maar, Germany. *Quat. Sci. Rev.* **2015**, *122*, 192–206. [CrossRef]
76. Krüger, S.; Mortensen, M.F.; Dörfler, W. Sequence Completed—Palynological Investigations on Lateglacial/Early Holocene Environmental Changes Recorded in Sequentially Laminated Lacustrine Sediments of the Nahe Palaeolake in Schleswig-Holstein, Germany. *Rev. Palaeobot. Palynol.* **2020**, *280*, 104271. [CrossRef]
77. Timms, R.G.O.; Matthews, I.P.; Palmer, A.P.; Candy, I.; Abel, L. A High-Resolution Tephrostratigraphy from Quoyloo Meadow, Orkney, Scotland: Implications for the Tephrostratigraphy of NW Europe during the Last Glacial-Interglacial Transition. *Quat. Geochronol.* **2017**, *40*, 67–81. [CrossRef]
78. Abrook, A.M.; Matthews, I.P.; Milner, A.M.; Candy, I.; Palmer, A.P.; Timms, R.G.O. Environmental Variability in Response to Abrupt Climatic Change during the Last Glacial–Interglacial Transition (16–8 cal ka BP): Evidence from Mainland, Orkney. *Scott. J. Geol.* **2020**, *56*, 30–46. [CrossRef]
79. Timms, R.G.O.; Abrook, A.M.; Matthews, I.P.; Francis, C.P.; Mroczkowska, A.; Candy, I.; Brooks, S.J.; Milner, A.M.; Palmer, A.P. Evidence for Centennial-scale Lateglacial and Early Holocene Climatic Complexity from Quoyloo Meadow, Orkney, Scotland. *J. Quat. Sci.* **2021**, *36*, 339–359. [CrossRef]
80. Hajdas, I.; Ivy-Ochs, S.D.; Bonani, G.; Loiter, A.F.; Zolitschka, B.; Schlüchter, C. Radiocarbon Age of the Laacher See Tephra: 11,230 ± 40 BP. *Radiocarbon* **1995**, *37*, 149–154. [CrossRef]
81. Blockley, S.P.E.; Lane, C.S.; Lotter, A.F.; Pollard, A.M. Evidence for the Presence of the Vedde Ash in Central Europe. *Quat. Sci. Rev.* **2007**, *26*, 3030–3036. [CrossRef]
82. Blockley, S.P.E.; Ramsey, C.B.; Lane, C.S.; Lotter, A.F. Improved Age Modelling Approaches as Exemplified by the Revised Chronology for the Central European Varved Lake Soppensee. *Quat. Sci. Rev.* **2008**, *27*, 61–71. [CrossRef]
83. Kletetschka, G.; Vondrák, D.; Hruba, J.; Prochazka, V.; Nabelek, L.; Svitavská-Svobodová, H.; Bobek, P.; Horicka, Z.; Kadlec, J.; Takac, M.; et al. Cosmic-Impact Event in Lake Sediments from Central Europe Postdates the Laacher See Eruption and Marks Onset of the Younger Dryas. *J. Geol.* **2018**, *126*, 561–575. [CrossRef]
84. Mortensen, M.F.; Birks, H.H.; Christensen, C.; Holm, J.; Noe-Nygaard, N.; Odgaard, B.V.; Olsen, J.; Rasmussen, K.L. Lateglacial Vegetation Development in Denmark—New Evidence Based on Macrofossils and Pollen from Slotseng, a Small-Scale Site in Southern Jutland. *Quat. Sci. Rev.* **2011**, *30*, 2534–2550. [CrossRef]
85. Larsen, J.J.; Noe-Nygaard, N. Lateglacial and Early Holocene Tephrostratigraphy and Sedimentology of the Store Slotseng Basin, SW Denmark: A Multi-Proxy Study: Lateglacial and Early Holocene Tephrostratigraphy and Sedimentology, SW Denmark. *Boreas* **2014**, *43*, 349–361. [CrossRef]
86. Candy, I.; Abrook, A.; Elliot, F.; Lincoln, P.; Matthews, I.P.; Palmer, A. Oxygen Isotopic Evidence for High-Magnitude, Abrupt Climatic Events during the Lateglacial Interstadial in North-West Europe: Analysis of a Lacustrine Sequence from the Site of Tirinie, Scottish Highlands. *J. Quat. Sci.* **2016**, *31*, 607–621. [CrossRef]
87. Housley, R.A.; MacLeod, A.; Nalepka, D.; Jurochnik, A.; Masojć, M.; Davies, L.; Lincoln, P.C.; Bronk Ramsey, C.; Gamble, C.S.; Lowe, J.J. Tephrostratigraphy of a Lateglacial Lake Sediment Sequence at Węgliny, Southwest Poland. *Quat. Sci. Rev.* **2013**, *77*, 4–18. [CrossRef]
88. Ringberg, B. *Beskrivning Till Jordartskartan Helsingborg SO*; Liber Distribution: Stockholm, Sweden, 1984.
89. Croudace, I.W.; Rindby, A.; Rothwell, R.G. ITRAX: Description and Evaluation of a New Multi-Function X-Ray Core Scanner. *Geol. Soc. Lond. Spec. Publ.* **2006**, *267*, 51–63. [CrossRef]

90. Aitchison, J. *The Statistical Analysis of Compositional Data*; Monographs on Statistics and Applied Probability; Chapman & Hall Ltd.: London, UK, 1986.
91. Kucera, M.; Malmgren, B.A. Logratio Transformation of Compositional Data. *Mar. Micropaleontol.* **1998**, *34*, 117–120. [CrossRef]
92. Weltje, G.J.; Tjallingii, R. Calibration of XRF Core Scanners for Quantitative Geochemical Logging of Sediment Cores: Theory and Application. *Earth Planet. Sci. Lett.* **2008**, *274*, 423–438. [CrossRef]
93. Heiri, O.; Lotter, A.F.; Lemcke, G. Loss on Ignition as a Method for Estimating Organic and Carbonate Content in Sediments: Reproducibility and Comparability of Results. *J. Paleolimnol.* **2001**, *25*, 101–110. [CrossRef]
94. Turney, C.S.M. Extraction of Rhyolitic Component of Vedde Microtephra from Minerogenic Lake Sediments. *J. Paleolimnol.* **1998**, *19*, 199–206. [CrossRef]
95. Dugmore, A.J.; Larsen, G.; Newton, A.J. Seven Tephra Isochrones in Scotland. *Holocene* **1995**, *5*, 257–266. [CrossRef]
96. Hayward, C. High Spatial Resolution Electron Probe Microanalysis of Tephras and Melt Inclusions without Beam-Induced Chemical Modification. *Holocene* **2012**, *22*, 119–125. [CrossRef]
97. Blaauw, M.; Christen, J.A. Flexible Paleoclimate Age-Depth Models Using an Autoregressive Gamma Process. *Bayesian Anal.* **2011**, *6*, 457–474. [CrossRef]
98. Fedotov, A.P.; Phedorin, M.A.; Enushchenko, I.V.; Vershinin, K.E.; Melgunov, M.S.; Khodzher, T.V. A Reconstruction of the Thawing of the Permafrost during the Last 170 Years on the Taimyr Peninsula (East Siberia, Russia). *Glob. Planet. Change* **2012**, *98–99*, 139–152. [CrossRef]
99. Kalugin, I.; Darin, A.; Rogozin, D.; Tretyakov, G. Seasonal and Centennial Cycles of Carbonate Mineralisation during the Past 2500 Years from Varved Sediment in Lake Shira, South Siberia. *Quat. Int.* **2013**, *290–291*, 245–252. [CrossRef]
100. Olsen, J.; Anderson, N.J.; Leng, M.J. Limnological Controls on Stable Isotope Records of Late-Holocene Palaeoenvironment Change in SW Greenland: A Paired Lake Study. *Quat. Sci. Rev.* **2013**, *66*, 85–95. [CrossRef]
101. Lauterbach, S.; Brauer, A.; Andersen, N.; Danielopol, D.L.; Dulski, P.; Hüls, M.; Milecka, K.; Namiotko, T.; Obremska, M.; Von Grafenstein, U.; et al. Environmental Responses to Lateglacial Climatic Fluctuations Recorded in the Sediments of Pre-Alpine Lake Mondsee (Northeastern Alps). *J. Quat. Sci.* **2011**, *26*, 253–267. [CrossRef]
102. Kylander, M.E.; Klaminder, J.; Wohlfarth, B.; Löwemark, L. Geochemical Responses to Paleoclimatic Changes in Southern Sweden since the Late Glacial: The Hässeldala Port Lake Sediment Record. *J. Paleolimnol.* **2013**, *50*, 57–70. [CrossRef]
103. Lowe, D.J.; Hogg, A.G.; Hendy, C.H. Detection of Thin Tephra Deposits in Peat and Organic Lake Sediments by Rapid X-Radiography and X-Ray Fluorescence Techniques. In Proceedings of the Tephra Workshop, Wellington, New Zealand, 30 June–1 July 1980; Victoria University of Wellington: Wellington, New Zealand, 1981; Volume 20, pp. 74–77.
104. Wastegård, S.; Veres, D.; Kliem, P.; Hahn, A.; Ohlendorf, C.; Zolitschka, B. Towards a Late Quaternary Tephrochronological Framework for the Southernmost Part of South America—The Laguna Potrok Aike Tephra Record. *Quat. Sci. Rev.* **2013**, *71*, 81–90. [CrossRef]
105. Høgaas, F.; Larsson, S.A.; Klug, M.; Olsen, L.; Wastegård, S. Palaeolake Sediment Records Reveal a Mid- to Late Younger Dryas Ice-sheet Maximum in Mid-Norway. *Boreas* **2022**, *51*, 41–60. [CrossRef]
106. Gehrels, M.J.; Newnham, R.M.; Lowe, D.J.; Wynne, S.; Hazell, Z.J.; Caseldine, C. Towards Rapid Assay of Cryptotephra in Peat Cores: Review and Evaluation of Various Methods. *Quat. Int.* **2008**, *178*, 68–84. [CrossRef]
107. Vogel, H.; Zanchetta, G.; Sulpizio, R.; Wagner, B.; Nowaczyk, N. A Tephrostratigraphic Record for the Last Glacial-Interglacial Cycle from Lake Ohrid, Albania and Macedonia. *J. Quat. Sci.* **2010**, *25*, 320–338. [CrossRef]
108. Kylander, M.E.; Lind, E.M.; Wastegård, S.; Löwemark, L. Recommendations for Using XRF Core Scanning as a Tool in Tephrochronology. *Holocene* **2012**, *22*, 371–375. [CrossRef]
109. Damaschke, M.; Sulpizio, R.; Zanchetta, G.; Wagner, B.; Böhm, A.; Nowaczyk, N.; Rethemeyer, J.; Hilgers, A. Tephrostratigraphic Studies on a Sediment Core from Lake Prespa in the Balkans. *Clim. Past* **2013**, *9*, 267–287. [CrossRef]
110. Kolling, H.; Bauch, A.H. A Stratigraphical-Sedimentological Study of the Last Interglacial Period in the Central Nordic Seas on the Basis of XRF Core Scanning. *Polarforschung* **2017**, *87*, 15–22. [CrossRef]
111. Peti, L.; Augustinus, P.C.; Gadd, P.S.; Davies, S.J. Towards Characterising Rhyolitic Tephra Layers from New Zealand with Rapid, Non-Destructive μ-XRF Core Scanning. *Quat. Int.* **2019**, *514*, 161–172. [CrossRef]
112. Balascio, N.L.; Francus, P.; Bradley, R.S.; Schupack, B.B.; Miller, G.H.; Kvisvik, B.C.; Bakke, J.; Thordarson, T. Investigating the Use of Scanning X-Ray Fluorescence to Locate Cryptotephra in Minerogenic Lacustrine Sediment: Experimental Results. In *Micro-XRF Studies of Sediment Cores*; Developments in Paleoenvironmental Research; Springer: Dordrecht, The Netherlands, 2015; Volume 17, pp. 305–324.
113. Björck, S.; Rundgren, M.; Ingólfsson, Ó.; Funder, S. The Preboreal Oscillation around the Nordic Seas: Terrestrial and Lacustrine Responses. *J. Quat. Sci.* **1997**, *12*, 455–465. [CrossRef]
114. Björck, S.; Muscheler, R.; Kromer, B.; Andresen, C.S.; Heinemeier, J.; Johnsen, S.J.; Conley, D.; Koç, N.; Spurk, M.; Veski, S. High-Resolution Analyses of an Early Holocene Climate Event May Imply Decreased Solar Forcing as an Important Climate Trigger. *Geology* **2001**, *29*, 1107. [CrossRef]
115. Staff, R.A.; Liu, R. Radiocarbon Calibration: The next Generation. *Sci. China Earth Sci.* **2021**, *64*, 507–510. [CrossRef]
116. Davies, S.J.; Lamb, H.F.; Roberts, S.J. Micro-XRF Core Scanning in Palaeolimnology: Recent Developments. In *Micro-XRF Studies of Sediment Cores*; Developments in Paleoenvironmental Research; Springer: Dordrecht, The Netherlands, 2015; Volume 17, pp. 189–226.